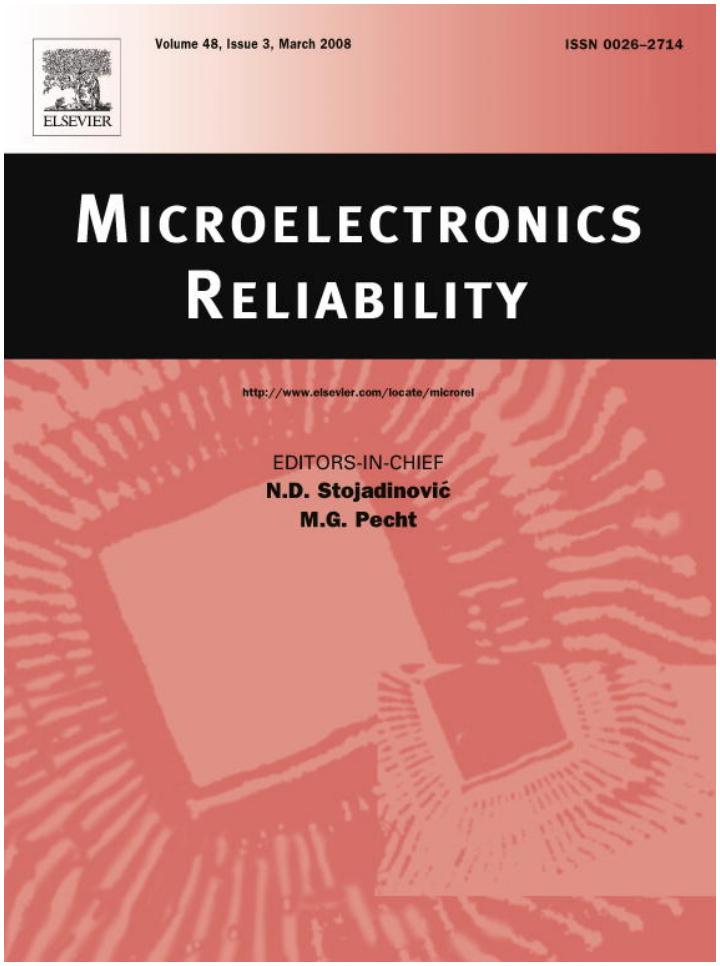

Available online at www.sciencedirect.com
ScienceDirect
Microelectronics Reliability 48 (2008) 416–424
MICROELECTRONICS RELIABILITY
www.elsevier.com/locate/microrel

Growth behavior of Cu/Al intermetallic compounds and cracks in copper ball bonds during isothermal aging

C.J. Hang [a,b,*], C.Q. Wang [a], M. Mayer [b], Y.H. Tian [a], Y. Zhou [b], H.H. Wang [c]

[a] State Key Laboratory of Advanced Welding Production Technology, Harbin Institute of Technology, Harbin 150001, China
[b] Centre for Advanced Materials Joining, University of Waterloo, Waterloo, Ontario, Canada N2L 3G1
[c] Nantong Fujistu Microelectronics Co. Ltd., Jiangsu 226001, China

Received 5 April 2007; received in revised form 23 May 2007
Available online 13 August 2007

Abstract

Copper wires are increasingly used in place of gold wires for making bonded interconnections in microelectronics. There are many potential benefits for use of copper in these applications, including better electrical and mechanical properties, and lower cost. Usually, wires are bonded to aluminum contact pads. However, the growth of Cu/Al intermetallic compounds (IMC) at the wire/pad interfaces is poorly understood, and if excessive would increase the contact resistance and degrade the bond reliability.

To study the Cu/Al IMC growth in Cu ball bonds, high temperature aging at 250 °C for up to 196 h has been used to accelerate the aging process of the bonds. The Cu/Al IMCs growth behavior was then recorded and the IMC formation rate of $6.2 \pm 1.7 \times 10^{-14}$ cm^2/s was obtained. In addition to the conventional *yz*-plane cross-section perpendicular to the bonding interface, a *xy*-plane cross-section parallel through the interfacial layers is reported. Three IMC layers were distinguished at the Cu/Al interfaces by their different colors under optical microscopy on the *xy*-plane cross-sections of ball bonds. The results of micro-XRD analysis confirmed that Cu_9Al_4, and $CuAl_2$ were the main IMC products, while a third phase is found which possibly is CuAl. During the aging process, IMC film growth starts from the periphery of the bond and propagates inward towards the centre area. Subsequently, with increased aging time, cavities are observed to develop between the IMC layer and the Cu ball surface, also starting at the bond periphery. The cavitation eventually links up and progresses toward the centre area leading to a nearly complete fracture between the ball and the intermetallic layer, as observed after 81 h.

1. Introduction

In microelectronic packaging, wire bonding is the predominant method for making electrical connections between chips and lead frames. Gold wire is the most popular interconnection material used in the wire bonding process. However, many studies have shown that reliability and durability problems exist with bonded assemblies under thermal exposure, due to metallurgical degradation of the wire/pad interface and void formation. Demands for better interconnection reliability is one of several factors forcing more attention on copper wire bonding. The advantages of copper wire bonding over gold wire bonding have been reported extensively [1–4]. Compared to gold or aluminum, copper has better mechanical, electrical, and thermal properties. Hence, copper wires could serve as an alternative to gold wires in high power interconnections and fine pitch bonding applications. Furthermore, because of the lower interdiffusion rate between the copper and the aluminum, copper bonds potentially have higher durability than gold bonds [5].

A limited amount of interfacial IMC formation in dissimilar metal ultrasonic or thermosonic wire bonds

* Corresponding author. Address: Centre for Advanced Materials Joining, University of Waterloo, Waterloo, Ontario, Canada N2L 3G1. Tel.: +1 5198884567x33326; fax: +1 5198886197.
E-mail addresses: c2hang@engmail.uwaterloo.ca, hangcj@hit.edu.cn (C.J. Hang).

0026-2714/$ - see front matter © 2007 Elsevier Ltd. All rights reserved.
doi:10.1016/j.microrel.2007.06.008

increases the bond strength [1]. But excessive IMC formation could result in the performance degradation of the bond. Increased thickness of IMC would produce higher electrical resistance, leading to a higher heat generation when current flows. This results in a multiplier effect, as the formation of additional IMC in the bonded interface is promoted by the heating due to elevated resistivity. In the Au/Al system, IMCs are easily formed in the bonded interface. Studies of Murali et al. [5] showed that a thick Au/Al IMC layer could easily form in a few hours of heating the gold ball bonds at 175–200 °C, which is the typical post mold curing temperature. Compared to the rapid growth of Au/Al IMC, the Cu/Al IMC growth has been suggested to be much slower. Previous researchers have observed no Cu/Al IMC in the as-bonded copper ball bonds even though a strong solid state weld existed [6,7]. Several days at the mold temperature or even at any higher temperature were suggested to be required to develop the Cu/Al IMCs in the interface [8,9]. Studies of Kim et al. showed that the growth rate of Cu/Al IMC was about 1/10 of that of Au/Al in the temperature range of 150–300 °C [10]. The atomic properties of copper, gold, and aluminum could explain the big difference in the IMCs growth. Compared to gold atoms, copper atoms have a greater atomic size misfit in the aluminum lattice and a lower electronegativity, hence making the formation of Cu/Al IMCs more difficult [5].

Because of the rapid growth of the Au/Al IMC, it is convenient to obtain a thick IMC layer in the gold ball bond for phase identification. However, the identification of the Cu/Al IMC phases in copper ball bonding has been suggested to be more difficult [11,12]. Due to the slow IMC growth, the amount of Cu/Al IMC has been found insufficient to be detected by conventional analysis equipment. Heretofore, the expected Cu/Al IMC phases in copper ball bonds have not been well confirmed. Fig. 1 shows the binary phase diagram of the Cu–Al system. It can be observed that five IMCs, i.e., Cu_9Al_4, Cu_3Al_2, Cu_4Al_3, CuAl, and $CuAl_2$ can be formed at temperatures from 150 to 300 °C [11,13].

Intermetallic phases between thin films share similarities with IMC formation in ball bonds [14]. Many researchers have focused attention on diffusion couples to facilitate these studies, in which Cu_9Al_4, CuAl, and $CuAl_2$ are identified [13,15,16].

Jin et al. reported that CuAl and $CuAl_2$ were the main phases in the Cu/Al bonds based on micro-XRD analysis results on bond fracture surfaces after aging temperatures from 150 to 200 °C [17]. Kim et al. also used the micro-XRD to identify the Cu/Al IMC phases on fractured pads and balls after ball shear testing. It was reported that Cu_9Al_4 was the main phase in copper ball bonds after thermal annealing at the temperature range from 150 to 300 °C [10].

To further contribute to the knowledge about Cu/Al IMCs, a study of 250 °C isothermal aging of copper bump bonds on aluminum metallization pads is reported. The growth behavior of the Cu/Al IMCs and the cracks between copper ball surface and the IMC layer during aging was investigated in detail. The main IMC phases in the copper bonds have also been determined using micro-XRD.

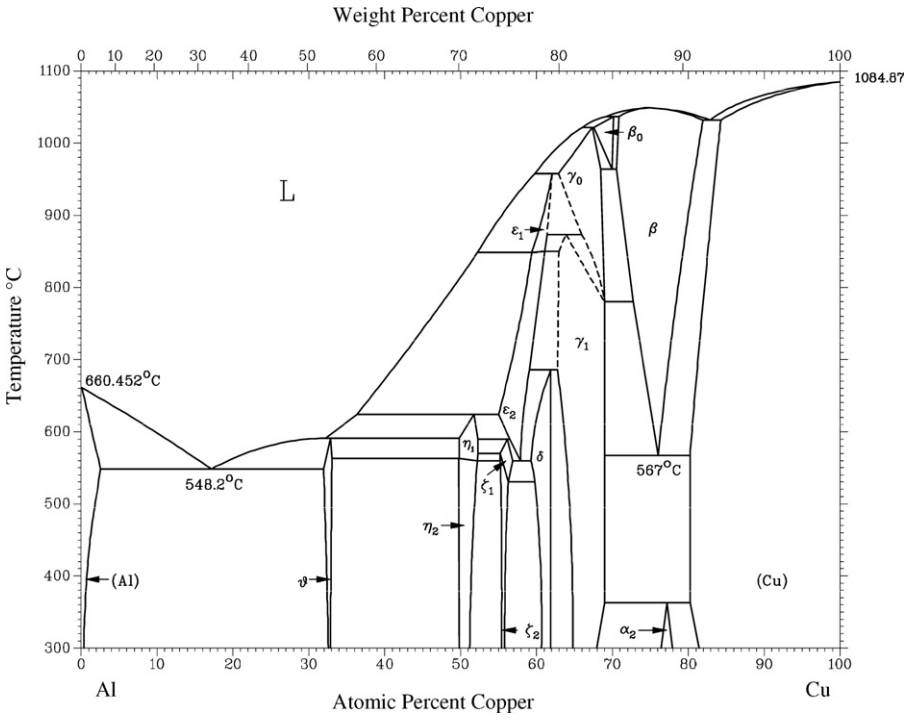

Fig. 1. Phase diagram of Cu–Al system [11].

2. Experimental

The ball bonds studied in this work were bonded on the silicon chips designed for power devices, with a 3 μm Al–1 wt.% Si–0.5 wt.% Cu metallization layer, attached to SOL 8 copper-type leadframes prior to ball bonding. A 50.4 μm (2 mil) diameter copper wire of 99.99 wt.% purity, with a break load range of 40–55 g and an elongation range of 20–30%, was used. The process was carried out by an ASM Eagle 60 ball/wedge bonder with an ultrasonic frequency of 138 kHz. In order to protect the copper free air balls (FAB) from oxidization during the electrical flame off process, a protective shielding gas, 95% N_2+5% H_2, was used with a flow rate of 0.8 l/min. The FABs with a nominal size of 100.8 μm (4 mil) were achieved with a current of 120 mA and arc time of 1 ms. The detailed bonding parameters are listed in Table 1 for reference. Table 2 shows the average characteristics of 20 copper bump bonds. To ensure sufficient material for subsequent cross-sectioning, more than 60 copper bump bonds were bonded on each chip. Fig. 2 shows a chip after the bonding process. The bonds were encapsulated in the EME-G700 green mold compound from Sumitomo Bakelite Co. Ltd. and then aged at 250 °C for 1–196 h in a Despatch custom thermal oven. This green mold compound has a halogen content of less than 1000 ppm. Hence the effect caused by halogen to the IMC growth is assumed to be negligible in this study. Then the samples were cooled down to room temperature in air. They were then re-mounted in epoxy resin and cross-sectioned with standard metallographic techniques.

The bonds were cross-sectioned in two different directions. Fig. 3 shows a three-dimensional schematic of the copper bond on the pad. The cross-sections in the *yz*-plane were carried out for IMC thickness measurement and also for investigation of the IMC growth behavior. The cross-sections in the *xy*-plane were then used for the micro-XRD analysis. Being parallel to the bonded interface, the *xy*-plane cross-section through the IMC layer provided a greater area of IMCs for micro-XRD analysis. The colors of the IMCs, which are different from those of Al, Si, and Cu under optical microscopy, were used as a reference to determine whether the cross-section was just inside the IMC layers.

Table 1
Bonding parameters of copper bump bonds

Bond parameter	Value
Standby power (mW)	60
Contact time (ms)	2
Contact power (mW)	60
Contact force (gf)	280
Bond time (ms)	25
Bond power (mW)	220
Bond force (gf)	80
Bonding temperature (°C)	220

Table 2
Characteristics of copper bonds

	Ball height (μm)	Shear force (gf)	Bond diameter (μm)	Shear strength (MPa)
Max	31.6	177	132	136.1
Min	26.7	131	123.5	100.3
Average	29.5	154.2	128	119.9
SD	1.4	10.3	2.5	8.1

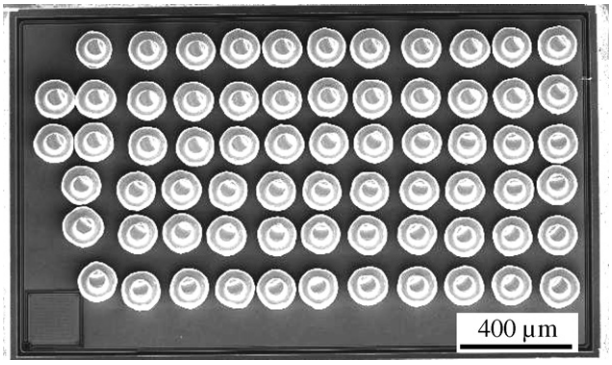

Fig. 2. Top view of the copper bump bonds on the Al metallization pad.

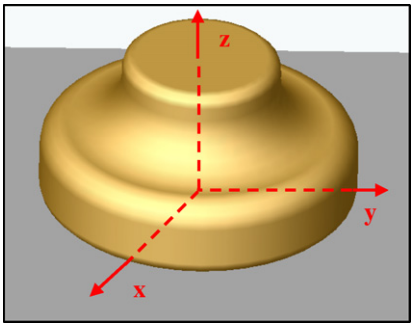

Fig. 3. Three-dimensional schematic of the copper bump bond.

A JSM-6310F scanning electron microscope (SEM), equipped with energy dispersive X-ray spectroscopy (EDX), was used to investigate the Cu/Al IMCs. The back scattered electron (BSE) mode was used for imaging. Analytical software for the measurement on the SEM images was used to evaluate the thickness of IMC layers and the crack length. Thickness measurements were performed primarily in the peripheral region of bonds, where the IMCs formed initially. Each reported IMC thickness was determined by an average of 15–20 points of measurement. The measurements of the crack length were performed along the bonding interface direction. The reported crack length was the average of six to eight measurement points. A RIKAGU D/MAX-3C XRD with a fine collimator of 50 μm in diameter was used for the analysis on the *xy*-plane cross-sections of the copper ball bonds. The identification of Cu/Al IMC phases was carried out by matching the micro-XRD results to the Joint Committee on Powder Diffraction Standards (JCPDS) database using the supplementary built-in software in the micro-XRD machine.

3. Results

3.1. Cu/Al IMC and crack growth behavior

An *yz*-plane cross-section image of a typical copper bump bond before thermal aging is shown in Fig. 4. The as-bonded joint assemblies were found to be free of voids or cracks. The deformation of the balls and pads during bonding is related to the capillary geometry as well as to the bonding conditions. Due to the geometry of the capillary, the maximum stress normally appears adjacent to its inner chamfer where the outer radius concentrates the stress during the ball bonding process [18]. Hence, the Al pad at the periphery of the bond undergoes severe deformation and is squeezed out. Furthermore, some aluminum is squeezed to the centre area forming a hill between the bond bottom and the aluminum pad, as shown in Fig. 4. Possibly Cu/Al IMCs have formed right after bonding and can be found if other advanced analysis techniques are used. However, no Cu/Al IMC is found in the bonded interface from this SEM image.

Fig. 5 shows the overall *yz*-plane cross-section images at the bonding interface in various copper bonds after aging at 250 °C with various aging periods. After 1 h of aging, a small amount of IMC was seen at the ball bond periphery. As marked with a white ellipse in Fig. 5a, the color of the IMC was different from both copper and aluminum, which is consistent with the observations of [7]. After 4 h of aging, as shown in Fig. 5b, the IMC developed both laterally and vertically. Furthermore, some cavities began to occur between the IMC layer and the bottom of the copper ball surface. As the aging time increased, the cavities grew inward towards the bond centre area in step with the development of the IMC, as shown in Fig. 5c. After 49 h of aging, a Cu/Al IMC layer was seen covering the whole bonded interface. Meanwhile, the cavities continued to grow and became cracks as a result. An annular gap was thereby formed between the copper ball surface and the IMC layer, as shown in Fig. 5d.

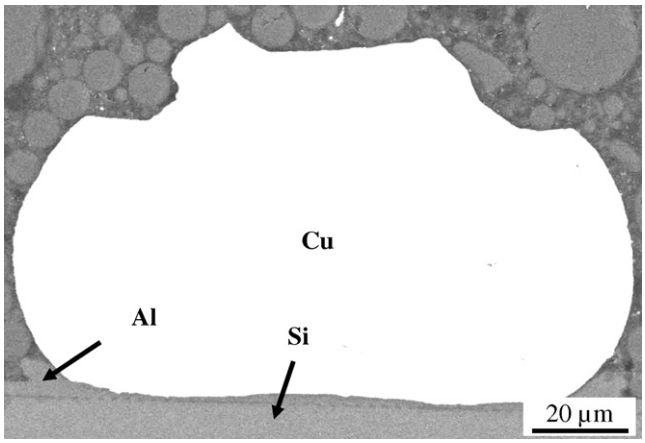

Fig. 4. SEM image of the *yz*-plane cross-section of copper bump bond before aging.

After 64 h of aging, the Cu/Al IMC growth slowed down and the annular gap continued to grow inward to the bond centre area as shown in Fig. 5e. After 81 h of aging, a complete fracture had formed between the copper ball bottom surface and the IMC layer. In this case, the copper ball was separated completely from the bonded interface, as shown in Fig. 5f. Fig. 5g shows the cross-section images of the copper bond after 169 h of aging. Compared to Fig. 5f, there was no significant difference except for a bigger fracture in the bonding interface. The growth behavior of the Cu/Al IMC at 250 °C could be described by the schematic diagram in Fig. 6.

3.2. Cu/Al IMC and crack growth rate

To investigate the Cu/Al IMC growth rate, the IMC layer thicknesses were measured after various aging times. The measured layer thickness of the IMC is plotted in Fig. 7a. It was clear that a high IMC growth rate occurs at the early stage, and as the aging time increases, the growth rate decreases gradually. After the formation of the complete fracture, the growth of the IMC layer stops.

In fact, the growth rate of an intermediate phase during the interdiffusion of metals follows the parabolic rate law and can be described with empirical equation [10,19,20]:

$$\delta = (Kt)^{\frac{1}{2}} \tag{1}$$

where δ is the thickness of the IMC layer; K indicates the reaction rate of IMC formation, and t represents the aging time.

The thickness of Cu/Al IMC versus square root of aging time for times smaller than 100 h is shown in Fig. 7b. This draft can be well fitted by a straight line with a correlation coefficient of 0.97. With Eq. (1) the reaction rate of the Cu/Al IMC formation is calculated. At 250 °C, the K of Cu/Al IMC is $6.2 \pm 1.7 \times 10^{-14}$ cm^2/s, which compares with 6.833×10^{-14} cm^2/s in [10].

The total lengths of the cracks in the bonds with various aging times have been measured, as plotted in Fig. 8. There are no cracks or cavities before 4 h aging. After 81 h, the cracks link up to be a complete fracture between the ball surface and the IMC layers and the crack growth stops.

3.3. Cu/Al IMC phase identification

Fig. 9 shows part of the *yz*-plane cross-section image of a copper bond after 64 h of isothermal aging at 250 °C. Judging from the different colors of IMCs, the whole IMC is comprised of three layers of differing composition. EDX analysis was performed on these three layers from layer A to layer C in Fig. 9. The EDX results listed in Table 3 suggest that the atomic ratios of copper and aluminum in these layers are: 1:2, 1:1, and 9:4, respectively. This result together with information from previous studies, as listed in Table 4 [6], leads to the deduction that the IMC phases present are $CuAl_2$, CuAl, and Cu_9Al_4, respectively.

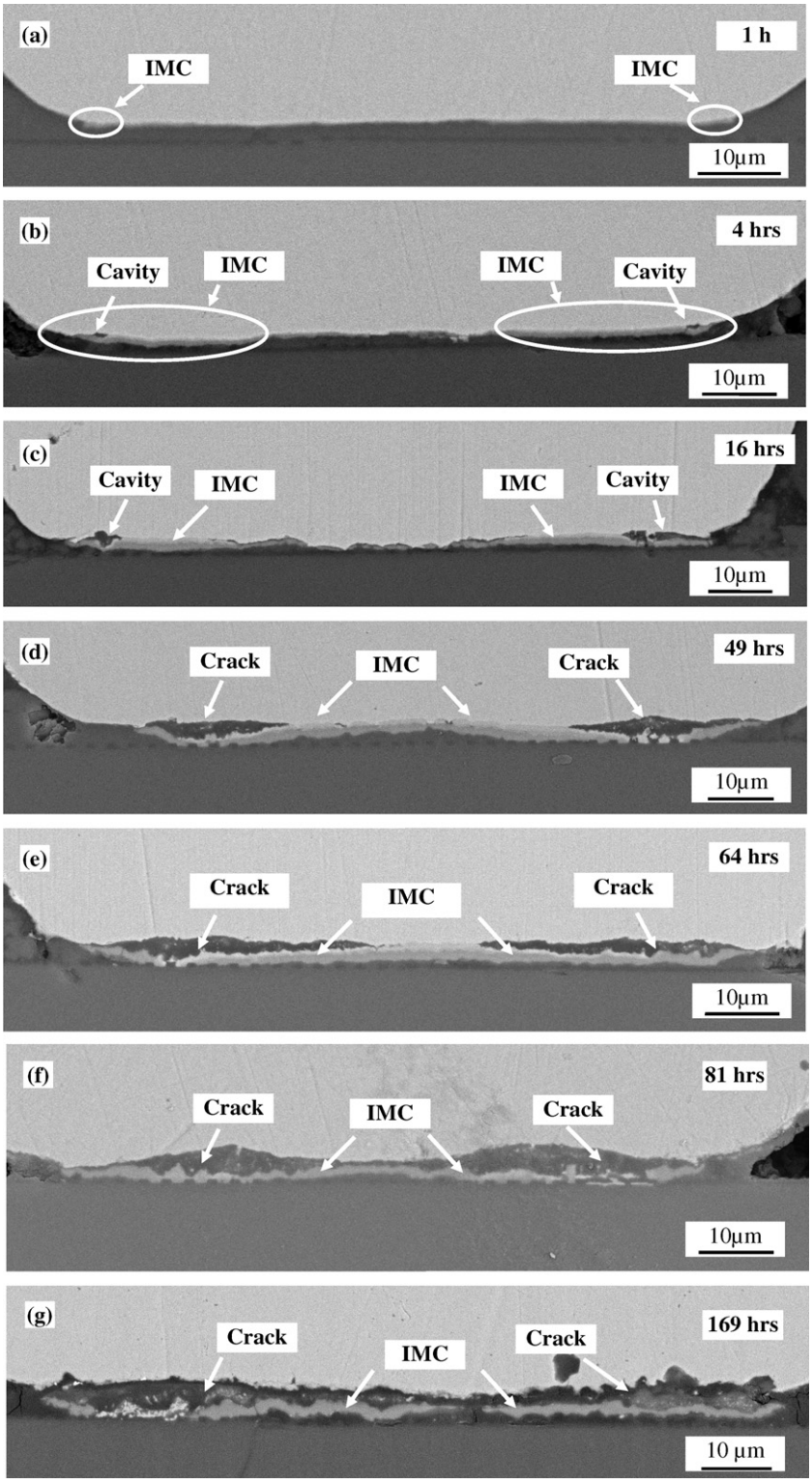

Fig. 5. The evolution of the Cu/Al IMC in the copper bump bonds at 250 °C after aging for 1, 4, 16, 49, 64, 81, and 169 h.

Fig. 10a shows an optical image of the *xy*-plane cross-section of a copper ball bond after 64 h of aging at 250 °C. Two different colored IMC phases can be seen in this image. The EDX results on these two phases showed the atomic ratios of copper and aluminum at 1:2 and 9:4, as shown in Fig. 10b. Combining this data with the EDX results in Table 3, the phase in the centre area appeared to correspond to layer A and the other to layer C as defined in Fig. 9. The third IMC phase, which is in layer B, is small in quantity and of a color close to the other phases. Therefore, it would be difficult to find in the optical image.

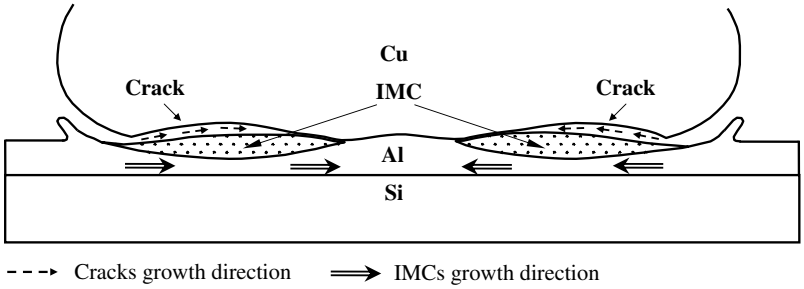

Fig. 6. Schematic showing the growth of IMCs and cracks in the copper bump bond during aging at 250 °C.

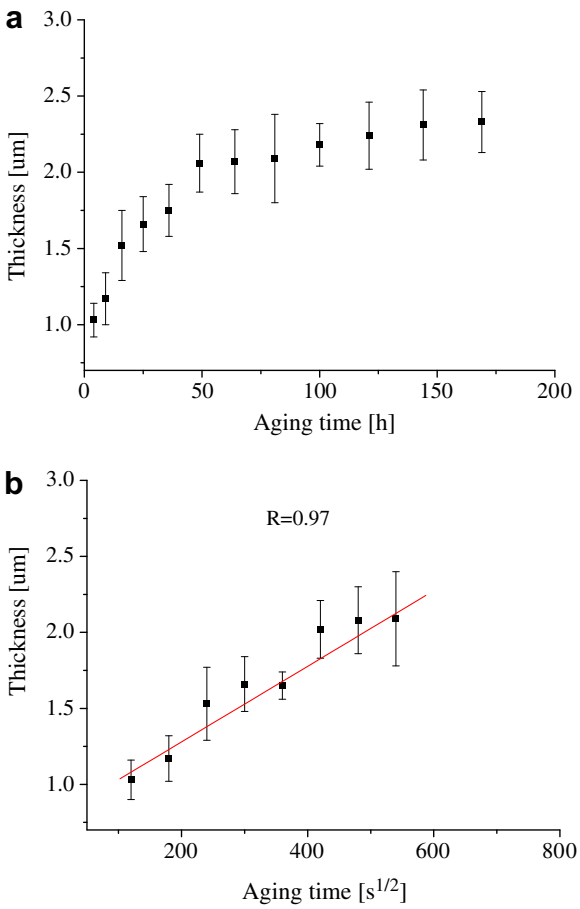

Fig. 7. (a) IMC thickness versus aging time [h] and (b) IMC thickness versus square root of the aging time [$s^{1/2}$] (less than 100 h).

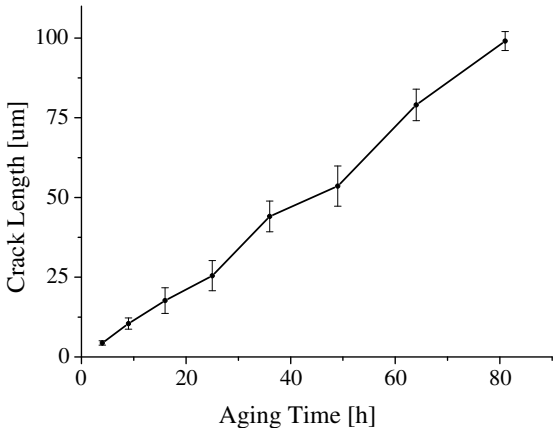

Fig. 8. Crack length versus aging time (4–81 h).

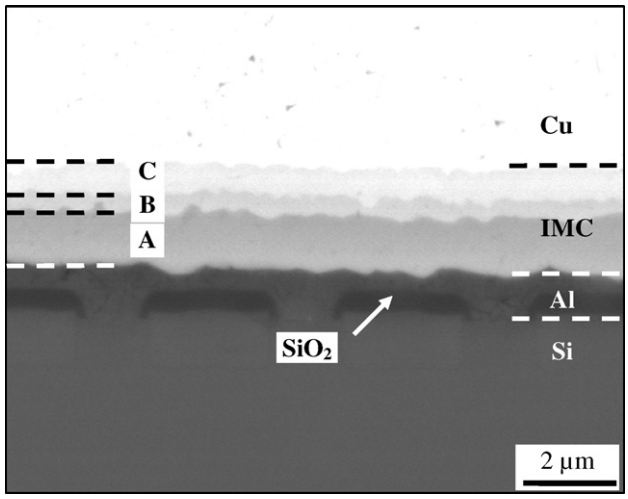

Fig. 9. SEM image of *yz*-plane cross-section of copper bump bond after 64 h aging at 250 °C.

In order to further identify these two main Cu/Al IMC phases, micro-XRD was performed on the *xy*-plane cross-sections of the copper ball bonds, as shown in Fig. 11. The result showed a much stronger Cu/Al IMC signal than obtained in previous studies [10,17]. Matching the micro-XRD results to the JCPDS cards, it is clear that the peaks located at 25.5°, 44.4°, and 81.5° agree well with the characteristics of Cu_9Al_4. Compared with the EDX results in Fig. 10b, this phase was confirmed to be Cu_9Al_4. The other phase with the peaks located at 43.0°, 47.5°, and 56.4°, was confirmed to be $CuAl_2$. According to the EDX results in Table 3 and the above mentioned studies, the third IMC phase, which is difficult to see in the *xy*-plane cross-section, was believed to be CuAl.

Table 3
EDX results on the IMC layers after 64 h aging at 250 °C

	Concentration (at.% Cu)	Ratio to Al (at.)	Predicted phases
A	33.4	1:2	$CuAl_2$
B	51.8	1:1	CuAl
C	68.4	9:4	Cu_9Al_4

Table 4
Selected characteristics of copper intermetallic compounds [6]

Phase	Concentration (at.%)	Crystal
Al	0.0–2.84	Cubic
$CuAl_2$	31.9–33.0	Tetragonal
CuAl	49.8–52.3	Mono
Cu_4Al_3	55.2–56.3	Mono
Cu_3Al_2	59.3–61.9	Trigonal
Cu_9Al_4	62.5–69	Cubic
Cu	80.3–100	Cubic

4. Discussion

The IMC growth behavior of Cu ball bonds on Al pads shows some difference from that of Au ball bonds, which is assumed to be due to the differences in their respective atomic properties [5]. It is reported that the growth rate of the Au/Al IMCs is more than 10 times higher than that of the Cu/Al IMCs [10]. In the Au/Al bonds, immediately after bonding, it is normal to observe considerable quantities of Au/Al IMCs formed in the bonded interface. In fact, in some production processes, bonds are acceptable only if they display more than 70% IMC coverage in the interfacial area [18]. During the bonding process, initial intermetallic forms as discrete islands across the diameter of the Au ball bond. With increased aging time, Au/Al IMC grows vertically and laterally on the bonded interface [14].

In the Cu/Al bonds, no Cu/Al IMC is observed in the as-bonded copper bonds even though high bond strength is normally obtained [7]. However, the Cu/Al IMCs can be observed in the bonded interface after some high temperature aging [6,7,10]. In this study, as shown in Fig. 5, some Cu/Al IMC is visible at the ball periphery after more than 1 h of aging at 250 °C. As the aging time increases, the Cu/Al IMC develops inward to the centre area and eventually forms a complete IMC layer between the bond and the pad. Because of the slow growth rate, the IMC evolution, including its initiation, is relatively easy to observe in the Cu/Al case. By comparison, it is difficult to observe the initial growth of the IMC in the Au/Al bond due to its fast growth rate during the bonding process.

It is believed that the shape of the Cu/Al IMC distribution at the ball periphery is related to the ball bonding process. During the bond formation, the ball bond undergoes severe deformation [3]. The maximal deformation in the bonding interface occurs at its periphery. That is one of the main reasons why the micro-welds initiate from the ball periphery [21]. As a consequence, deformation microstructure features, for instance, cells, dislocations, and slip bands [3] are formed near the bond interface, especially at the ball periphery. These features have similar effect as vacancies on the interdiffusion. Additionally, there is considerable energy stored in these severe deformation areas after bonding. Furthermore, the non-uniform ball

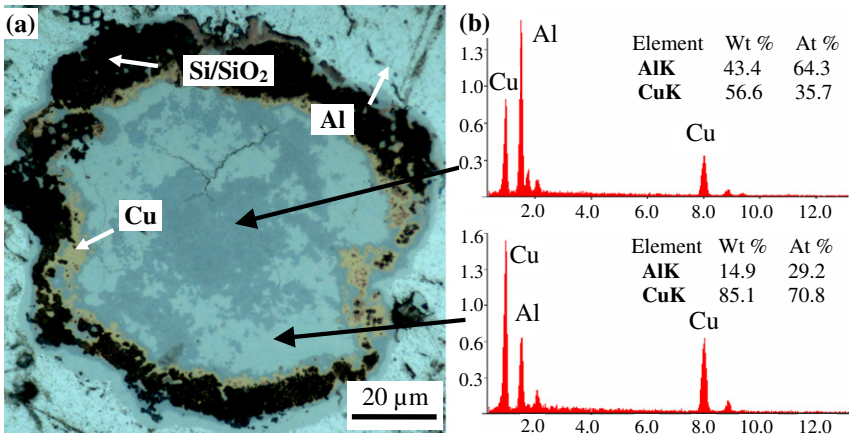

Fig. 10. (a) Optical image of the *xy*-plane cross-section in the IMC layers of the copper bump bond after aging at 250 °C for 64 h and (b) the energy spectrum.

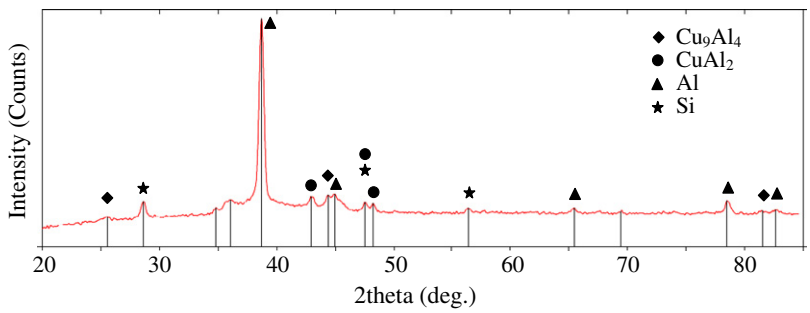

Fig. 11. Micro-XRD result of the IMCs in the copper bump bond after 64 h aging at 250 °C.

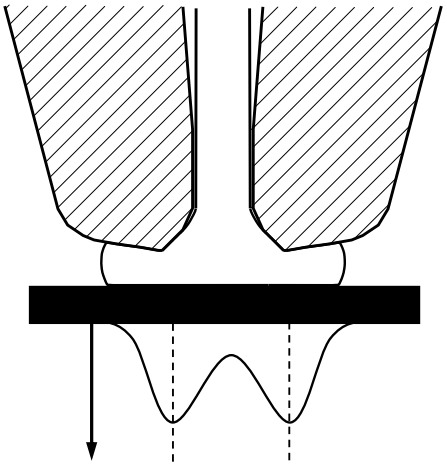

Fig. 12. Schematic of residual stress distribution for ball bond/substrate interface (compare [23]).

deformation and the dissimilarity of wire and substrate materials lead to a non-uniform residual stress distribution in the bond. During bonding, the contact between the ball and pad is produced by the elastic or elastoplastic deformation, where the tensile stress occurs at the edge of the contact area [21,22]. After bonding, a residual stress remains around the contact-interface. According to the observation of Chen et al. the maximum residual stress gradient under pad occurs at the bond periphery, as reproduced schematically in Fig. 12 [23].

The deformation microstructures, stored energy and the non-uniform residual stress distribution are expected to facilitate the Cu/Al IMC initial growth from the ball periphery. It is well accepted that the deformed microstructures decrease the activation energy of the metal atoms for interdiffusion and thus are beneficial to the IMC formation. The deformed microstructures of the copper ball bond, which are most intense at the ball periphery, accelerate the interdiffusion of the Cu and Al atoms and facilitate the initial formation of the IMC in these areas. Furthermore, at a high temperature, the stored energy caused by deformation during bonding will be released to facilitate the interdiffusion and the IMC formation. In the copper ball bonds, more stored energy is released at the ball periphery and so the Cu/Al IMC grows initially from these areas.

An uneven distribution of the local stress (stress gradient) naturally implies a chemical potential gradient. This is a necessary stress condition to increase the diffusion rates of mobile species during accelerated isothermal aging [18,24]. Under elevated temperature, the solid state diffusion and phase formation are enhanced in regions with high stress gradients [11]. In the bonded interface, the greatest residual stress gradients occur at the ball periphery. Therefore, the IMC is apt to initiate from these areas.

The cavity growth, which follows the Cu/Al IMC growth, shows some similarities to the de-bonding ring growth in Au/Al bonds. With the growth of the IMC in the Au/Al bond, the partial de-bonding between the upper IMC layer and the gold ball develops from the ball periphery and grows inwards to the ball centre [14,18,25,26]. It is believed that the de-bonding is related to the interactions between the residual stresses in the bonded balls, intrinsic IMC growth stresses and the thermo-chemical degradation of the IMCs [18]. In the Cu/Al bond, the cavities initiate from the ball periphery after the IMC layers are substantially developed and then grow inward to the centre area. This is similar to the de-bonding ring growth behavior in Au/Al bond. It is also believed that the cavity growth behavior is related to the residual stresses and intrinsic IMC growth stresses. During the aging process at high temperature, significant internal stresses can be developed as a result of the reactive diffusion [18,27] between copper and aluminum. When the overall internal stresses developed during interdiffusion plus the residual stresses from the bonding process exceed the bond strength of one of the interfaces, the stresses would be released by plastic deformation or fracture. It has been observed that micro-cracks and voids in diffusion couples are also developed as a consequence [28]. In the Cu/Al bond, the IMC initiates at the ball periphery. As a result, higher internal stresses start to develop at these areas initially. The overall stresses eventually exceed the bond strength between the upper IMC layer and the ball bottom surface. At this point the cavities would develop from the Cu/Al bond periphery. With the growth of the IMC laterally and vertically, more internal stresses are produced to drive the cavities growing inward toward the bond centre area. Finally a complete fracture forms between the ball bond and the upper IMC layer.

In this study, the bonding parameters have been optimized to maximize bond strength while assuring specified bond dimensions. This process resulted in a thickness variation of the Al pad with thinned peripheral areas. If the bonding conditions were optimized to prevent the Al thinning, the bond reliability could possibly be improved.

In addition, no visible change of the external appearance of the packaged chip was found after aging. No void or mold compound delamination was observed in the cross-sectional samples. Therefore, outgassing, weight loss or other mold compound degradation mechanisms were not investigated in this study.

5. Conclusions

1. The Cu/Al IMC growth rate decreases gradually with the increase of aging time. The growth stops when the complete fracture forms between the copper ball surface and the IMC layer. The IMC growth obeys a parabolic law.
2. The main phases in the Cu/Al IMC were confirmed to be Cu_9Al_4, and $CuAl_2$. CuAl could be present in smaller amounts.
3. Cu/Al IMC forms initially at the bond periphery and develops inward towards the central area. Following the growth of the IMC, cavities also start to grow from

the ball periphery and extend inward towards the bond centre, finally forming a complete fracture between the copper ball bottom surface and the upper IMC layer.

Acknowledgement

This work has been supported by the Natural Sciences and Engineering Research Council (NSERC) of Canada.

References

[1] Harman G. Wire bonding in microelectronics, materials, processes, reliability, and yield. second ed. McGraw-Hill; 1997. p. 21.
[2] Nguyen Luu T, McDonald D, Danker AR, et al. Optimization of copper wire bonding on Al–Cu metallization. IEEE Trans Comp Pack Manuf Technol 1995;18(2):423.
[3] Murali S, Srikanth N, Vath III Charles J. Grains, deformation substructures, and slips bands observed in thermosonic copper ball bonding. Mater Charact 2003;50:39.
[4] Tan CW, Daud AR, Yarmo MA. Corrosion study at Cu–Al interface in microelectronics packaging. Appl Surf Sci 2002;191:67.
[5] Murali S, Srikanth N, Vath III Charles J. An analysis of intermetallics formation of gold and copper ball bonding on thermal aging. Mater Res Bull 2003;38(2):637.
[6] Wulff FW, Breach CD, Stephan D, et al. Characterisation of intermetallic growth in copper and gold ball bonds on aluminum metallisation. In: Proceedings of the sixth EPTC; 2004.
[7] Wulff FW, Breach CD, Stephan D, et al. Further characterization of intermetallic growth in copper and gold ball bonds on aluminum metallization. In: Proceedings of SEMICON; 2005.
[8] Harman G. Wire bonding in microelectronics. New York: McGraw-Hill; 1989. p. 135.
[9] Ellis TW, Levine L, Wicen R, et al. Copper wire bonding. In: Proceedings of SEMICON conference; 2000.
[10] Kim HJ, Lee JY, Paik KW, et al. Effects of Cu/Al intermetallic compound (IMC) on copper wire and aluminum pad bondability. Trans Comp Pack Technol 2003;26(2):367.
[11] Funamizu Y, Watanabe K. Interdiffusion in the Al–Cu system. Trans Jpn Inst Metal 1971;12:147.
[12] Braunovic M, Alexandrov N. Intermetallic compounds at aluminum to copper electrical interfaces: effect of temperature and electric current. IEEE Trans Comp Pack Manuf Technol 1994;A17:78.
[13] Tamou Y, Li J, Russell SW, et al. Thermal and ion beam induced thin film reactions in Cu–Al bilayers. Nucl Instrum Method Phys Res 1992;B64:130.
[14] Breach CD, Wulff FW. New observations on intermetallic compound formation in gold ball bonds: general growth patterns and identification of two forms of Au_4Al. Microelectron Reliab 2004;44:973.
[15] Rajan K, Wallach ER. A transmission electron microscopy study of intermetallic formation in aluminum–copper thin film couples. J Crystal Growth 1980;49:297.
[16] Hentzell HTG, Thompson RD, Tu KN. Interdiffusion in copper–aluminum thin film bilayers. I. Structure and kinetics of sequential compound formation. J Appl Phys 1983;54:6923.
[17] Jin O, Masahiro K, Isao A. Investigation of the reliability of copper ball bond to aluminum electrodes. IEEE Trans Comp Hybr Manuf Technol 1987;4:550.
[18] Breach CD, Wulff F, Tok CW. An unusual mechanical failure mode in gold ball bonds at 50 μm pitch due to degradation at the Au–Au_4Al interface during ageing in air at 175 °C. Microelectron Reliab 2006;46:543.
[19] Jang GY, Duh JG, Takahashi H, et al. Solid-state reaction in an Au wire connection with an Al–Cu pad during aging. J Electron Mater 2006;35(2):323.
[20] Philofsky E. Intermetallic formation in gold–aluminum systems. Solid State Electron 1970;13:1391.
[21] Lum I, Jung JP, Zhou Y. Bonding mechanism in ultrasonic gold ball bonds on copper substrate. Metall Mater Trans A 2005;A36:1279.
[22] Takahashi Y, Matsusaka S. Adhesional bonding of fine gold wires to metal substrates. Adhes Sci Technol 2003;17(3):435.
[23] Chen J, Degryse D, ratchev P, et al. Mechanical issues of Cu-to-Cu wire bonding. IEEE Trans Comp Pack Technol 2004;27(3):539.
[24] Schmalzried H. Chemical kinetics of solids. VCH Publishers; 1995.
[25] Carr CLJ. Accelerated testing of gold–aluminum ball bond. MSD dissertation, University of Waterloo, Canada; 2005.
[26] Breach CD, Wulff F, Calpito D. Degradation of the Au_4Al compound in gold ball bonds during isothermal aging in air at 175 °C. J Mater Sci 2004;31(19):6125.
[27] Philibert J. Reactive diffusion in thin films. Appl Surf Sci 1991;53:74.
[28] Beke DL, Szabó IA, Erdélyi Z, et al. Diffusion induced stresses and their relaxation. Mater Sci Eng A 2004;387–389:4.